
Research Articles: Systems/Circuits

Individual movement variability magnitudes are explained by cortical neural variability

Shlomi Haar^{1,4}, Opher Donchin^{2,4} and Ilan Dinstein^{3,1,4}

¹*Dept. of Brain and Cognitive Sciences, Ben-Gurion University of the Negev, Israel*

²*Dept. of Biomedical Engineering, Ben-Gurion University of the Negev, Israel*

³*Dept. of Psychology, Ben-Gurion University of the Negev, Israel*

⁴*Zlotowski Center for Neuroscience, Ben-Gurion University of the Negev, Israel*

DOI: 10.1523/JNEUROSCI.1650-17.2017

Received: 13 June 2017

Revised: 19 July 2017

Accepted: 5 August 2017

Published: 18 August 2017

Author Contributions: S.H., O.D., and I.D., Conception and design, Interpretation of data, Drafting and revising the article; S.H., Data acquisition and analysis.

Conflict of Interest: The authors declare no competing financial interests.

We would like to thank Ilan Shelef and Moti Salti for their help in acquiring the fMRI data, and Lior Shmuelof for helpful discussions about the manuscript. The research described in this paper was supported by ISF grant 961/14 (I.D.), Helmsley Foundation (O.D.) and the ABC Robotics Center.

Corresponding author: Shlomi Haar (haar@post.bgu.ac.il; +972-8-6428766) Ben-Gurion University of the Negev, P.O.B. 653 Beer-Sheva, 8410501 Israel

Cite as: J. Neurosci ; 10.1523/JNEUROSCI.1650-17.2017

Alerts: Sign up at www.jneurosci.org/cgi/alerts to receive customized email alerts when the fully formatted version of this article is published.

Accepted manuscripts are peer-reviewed but have not been through the copyediting, formatting, or proofreading process.

Copyright © 2017 the authors

Individual movement variability magnitudes are explained by 1
cortical neural variability 2

Shlomi Haar^{1,4}, Opher Donchin^{2,4}, Ilan Dinstein^{3,1,4} 3

- 1. Dept. of Brain and Cognitive Sciences, Ben-Gurion University of the Negev, Israel 4
- 2. Dept. of Biomedical Engineering, Ben-Gurion University of the Negev, Israel 5
- 3. Dept. of Psychology, Ben-Gurion University of the Negev, Israel 6
- 4. Zlotowski Center for Neuroscience, Ben-Gurion University of the Negev, Israel 7

Corresponding author: Shlomi Haar (haar@post.bgu.ac.il ; +972-8-6428766) 9
 Ben-Gurion University of the Negev, P.O.B. 653 Beer-Sheva, 8410501 Israel 10

Author Contributions: S.H., O.D., and I.D., Conception and design, Interpretation of data, Drafting 11
 and revising the article; S.H., Data acquisition and analysis. 12

Abbreviate title: Relating neural and movement variability 14

Keywords: neural variability, movement variability, fMRI, motor control, motor system 16

Number of figures: 7 18

Number of words:	Abstract	180	19
	Introduction	646	20
	Discussion	1499	21

Conflict of Interest: The authors declare no competing financial interests. 23

Acknowledgements: We would like to thank Ilan Shelef and Moti Salti for their help in acquiring the fMRI 25
 data, and Lior Shmuelof for helpful discussions about the manuscript. The research described in this paper 26
 was supported by ISF grant 961/14 (I.D.), Helmsley Foundation (O.D.) and the ABC Robotics Center. 27

ABSTRACT 28

Humans exhibit considerable motor variability even across trivial reaching movements. This variability can be separated into specific kinematic components such as extent and direction, which are thought to be governed by distinct neural processes. Here, we report that individual subjects (males and females) exhibit different magnitudes of kinematic variability, which are consistent (within individual) across movements to different targets and regardless of which arm (right or left) was used to perform the movements. Simultaneous fMRI recordings revealed that the same subjects also exhibited different magnitudes of fMRI variability across movements in a variety of motor system areas. These fMRI variability magnitudes were also consistent across movements to different targets when performed with either arm. Cortical fMRI variability in the posterior-parietal cortex of individual subjects explained their movement-extent variability. This relationship was apparent only in posterior-parietal cortex and not in other motor system areas, thereby suggesting that individuals with more variable movement preparation exhibit larger kinematic variability. We, therefore, propose that neural and kinematic variability are reliable and interrelated individual characteristics that may predispose individual subjects to exhibit distinct motor capabilities.

Significance Statement: Neural activity and movement kinematics are remarkably variable. While this intertrial variability is mostly over looked, here we demonstrate that individual human subjects exhibit distinct magnitudes of neural and kinematic variability, which are stable across movements to different targets and when performing these movements with either arm. Furthermore, when examining the relationship between cortical variability and movement variability, we find that cortical fMRI variability in the parietal cortex of individual subjects explained their movement extent variability. Hence, we were able to explain why some subjects performed more variable movements than others based on their cortical variability magnitudes.

INTRODUCTION 52

Intertrial variability is a fundamental characteristic of human movements (e.g., Harbourne and Stergiou, 2009). Variability of specific kinematic components such as movement extent and movement direction is thought to be governed by independent neural processes (Gordon et al., 1994b; Krakauer et al., 2000; van Beers, 2009) according to the demands of the examined motor task (Todorov, 2004; Latash et al., 2007). While kinematic variability is detrimental for movement accuracy, it is thought to be critical for motor learning (Wilson et al., 2008; e.g., Braun et al., 2009; Teo et al., 2011; Herzfeld and Shadmehr, 2014; Wu et al., 2014).

Intertrial variability is also a fundamental characteristic of neural activity, which is apparent in the variable timing and amplitude of neural responses across trials containing an identical stimulus or task (Stein et al., 2005; Faisal et al., 2008; e.g., Churchland and Abbott, 2012; Dinstein et al., 2015; Sauerbrei et al., 2015). As with kinematic variability, intertrial neural variability also seems to be important for motor learning as demonstrated in studies with songbirds (Kao et al., 2005; Ölveczky et al., 2011; Woolley and Kao, 2015) and primates (Mandelblat-Cerf et al., 2009). Given that neural activity generates behavior, one may expect that intertrial variability in the activity of specific neural populations would generate corresponding intertrial variability in specific kinematic components of movement (e.g., movement extent and/or direction).

Studies that have examined this potential relationship have proposed three alternative theories. The first theory proposed that kinematic variability during visually guided movements is mostly explained by variability in sensory neural populations. For example, intertrial variability in the initial speed of smooth-pursuit eye movements can be explained by variability in the estimation of target speed in MT neurons (Osborne et al., 2005; for review, see Lisberger and Medina, 2015). In contrast, the second theory has proposed that kinematic variability during reaching movements is generated by variable preparatory (motor planning) activity of premotor and primary motor neurons (Churchland et al., 2006). Finally, the third theory has suggested that kinematic variability is caused by neural and neuro-muscular variability during actual movement execution (van Beers et al., 2004; van Beers, 2009). Taken together, these studies suggest that distinct neural variability sources are correlated with kinematic variability under different experimental conditions, which include the

sensory-motor requirements of the examined motor task (e.g., smooth-pursuit ocular movements 80
versus reaching movements) and the temporal structure of the task (e.g., imposing a delay between 81
movement planning and execution). 82

In the current study we examined several outstanding questions regarding kinematic 83
variability, neural variability, and their potential relationship in humans: 1. Do individual subjects 84
exhibit consistent magnitudes of kinematic variability regardless of the movements that they are 85
performing? 2. Do individual subjects exhibit consistent magnitudes of neural variability regardless 86
of the movements that they are performing? 3. If so, are between-subject differences in kinematic 87
variability explained by differences in neural variability in specific sensory and/or motor brain 88
areas? Answering these questions is critical for establishing that individual subjects exhibit 89
characteristic kinematic and neural variability magnitudes that may predispose them to exhibit 90
particular motor learning capabilities while also adding new insights regarding the potential 91
relationship between neural variability and kinematic variability. 92

To answer the questions above and relate the findings with the existing behavioral and 93
electrophysiology literature we quantified intertrial variability of movement direction, peak velocity, 94
and extent across slice (out-and-back) reaching movements. These movements were performed to 95
four peripheral targets with either right or left arm on a touch screen while brain activity was 96
recorded with fMRI. We then quantified fMRI response variability in the primary motor, premotor, 97
parietal, and visual brain areas of each subject and examined whether it was possible to explain 98
between-subject differences in kinematic variability according to neural variability magnitudes in 99
specific brain areas. Note that in our study all movements were performed without visual feedback to 100
preclude the potential influence of neural variability associated with visual input. 101

METHODS 102

Subjects. 32 right-handed volunteers with normal or corrected-to-normal visual acuity (15 103
 women and 17 men, aged 22-36 (25.6±2.5)) participated in the present study. The Soroka Medical 104
 Center Internal Review Board approved the experimental procedures and written informed consent 105
 was obtained from each subject. The sample size was selected so that the correlation effect size of 106
 0.4 would have power greater than $1 - \beta = 0.75$ (one-tailed test), with α set to 0.05. According to 107
 G*Power (Faul et al., 2009), the required minimum sample size is 30. 108

Experimental Setup and Design. Subjects lay in the scanner bore and viewed a back- 109
 projected screen through an angled mirror, which prevented any visual feedback of their arm and 110
 hand. An MRI-compatible digitizing tablet (Hybridmojo LLC, CA, USA) was placed over the 111
 subject's waist and used to track their arm movements (Figure 1A). Subjects performed slice (out- 112
 and-back) reaching movements from a central target to four peripheral targets located 7 and 13 cm 113
 from the central target in each of two directions, $\pm 45^\circ$ from the midline (Figure 1B). Subjects did not 114
 receive any visual feedback of their arm location during movement. Each trial started with the 115
 presentation of a peripheral target for one second. Four seconds after the target disappeared, the 116
 central target changed from red to green, indicating that the movement should be performed by 117
 moving the stylus pen on the tablet. Subjects had one second to complete the movement after which 118
 the center target turned red and remained red for the entire inter-trial-interval (ITI), which lasted six 119
 seconds. There was no post-trial visual feedback or knowledge-of-results. All subjects performed 120
 three experimental runs with each arm, each lasted 9 minutes and contained 11 movements to each 121
 of the four targets in a random order. The experiment started with three runs of the left (non- 122
 dominant) arm, followed by three runs of the right (dominant) arm. Subjects were trained on the task 123
 inside the scanner with both hands, before the scan, until they reported that they were comfortable 124
 performing it. 125

Movement Recording and Analysis. Kinematic data were recorded at 200 Hz. Trials with a 126
 reaction time of more than 1 second, trials with a movement angle error $>30^\circ$ (at peak velocity or 127
 end point), and trials with movement length that was $<50\%$ or $>200\%$ of the target distance were 128
 discarded from further analysis. Trials containing correction movements (i.e., velocity profiles with 129

more than two peaks) were also removed. On average approximately 8% (std 3%) of the trials were 130
discarded for each subject. There was no significant difference in the number of discarded trials 131
between the two arms. 132

We quantified intertrial variability for each of three kinematic components: movement 133
direction, movement extent, and peak movement velocity. Movement extent and peak velocity 134
variabilities were normalized by their respective means so as to compute the coefficient of variation 135
(CV). This was necessary, because the variability of these kinematic components scales with their 136
mean (speed-accuracy trade-off; Schmidt et al., 1979). Movement direction variability was 137
quantified by the standard deviation (SD) across trials. Each of these measures was computed for 138
each target and each subject separately and then averaged across targets to compute a single extent, 139
peak velocity, and direction variability measure for each subject. 140

MRI acquisition and preprocessing. Imaging was performed using a Philips Ingenia 3T MRI 141
scanner located at the Ben-Gurion University Brain Imaging Research Center. The scanner was 142
equipped with a 32 channel head coil, which was used for RF transmit and receive. Blood 143
oxygenation level-dependent (BOLD) contrast was obtained using a T2* sensitive echo planar 144
imaging (EPI) pulse sequence (TR = 2000 ms; TE = 35 ms; FA = 90°; 28 slices; voxel size of 145
2.6*2.6*3 mm and with 0.6 mm gap). Anatomical volumes were acquired with a T1-weighted 146
sagittal sequence (TR = 8.165 ms; TE = 3.74 ms; FA = 8°; voxel size of 1*1*1 mm). 147

MRI data were preprocessed with the Freesurfer software package 148
(<http://surfer.nmr.mgh.harvard.edu>, Fischl, 2012) and FsFast (Freesurfer Functional Analysis 149
Stream). Briefly, this process includes removal of non-brain tissue and segmentation of subcortical, 150
gray, and white matters based on image intensity. Individual brains were registered to a spherical 151
atlas which utilized individual cortical folding patterns to match brain geometry across subjects. 152
Each brain was then parcellated into 148 cortical ROIs using the Destrieux anatomical atlas 153
(Destrieux et al., 2010). Functional scans were subjected to motion correction, slice-timing 154
correction and temporal high-pass filtering with a cutoff frequency of two cycles per scan. 155
Functional scans were registered to the high-resolution anatomical volume. No additional spatial 156

smoothing was performed. Preprocessed data was imported into MATLAB (R2015a, *MathWorks Inc.* USA), and all further analysis was performed using custom software written in matlab.

Time course analysis. To ensure that our estimates of intertrial fMRI variability were not generated by head motion, respiration, and blood flow artifacts, we removed the following components from the fMRI time-course of each cortical voxel, through linear regression: (1) six head motion parameters obtained by rigid body correction of head motion (three translations and three rotations), (2) fMRI time-course from the lateral ventricles, and (3) the mean fMRI signal of the entire cortex (i.e., global component). In addition, we normalized the time-course of each voxel to a mean of zero and unit variance (i.e., Z-score). This ensured that overall time-course variance was equal across subjects such that our measure of inter-trial fMRI variability captured only task-related trial-by-trial variability differences across subjects rather than variability associated with the entire scanning session.

Identification of regions of interest. Visual and motor regions of interest (ROIs), in both left and right hemispheres, were defined a priori according to a combination of anatomical and functional criteria in the native space of each subject. We first used the automated Freesurfer parcellation pipeline to identify 148 anatomical ROIs in each of the subjects, based on the Destrieux anatomical atlas (Destrieux et al., 2010). We then selected the 100 continuous functional voxels that exhibited the strongest activation when contrasting all movement trials versus rest. To confine the ROIs to specific anatomical locations across all subjects, we selected the voxels within the following Freesurfer ROIs: Early visual cortex (Vis) - Occipital pole and calcarine sulcus; Superior parietal lobule (SPL) - Anterior portion of the superior parietal lobule, superior to the IPS and slightly posterior to the postcentral sulcus; Inferior parietal lobule (IPL) - Dorsal portion of the angular gyrus and the middle segment of the intraparietal sulcus; Primary motor cortex (M1) - anterior bank of the central sulcus in the hand knob area; Dorsal premotor cortex (PMd) - Junction of superior frontal sulcus and precentral sulcus; Ventral premotor cortex (PMv) - Junction of inferior frontal sulcus and precentral sulcus; and Supplementary motor area (SMA) - Medial wall of the superior frontal gyrus, anterior to the central sulcus, posterior to the vertical projection of the anterior commissure.

We also defined control ROIs that did not exhibit task-related activations in the dorsolateral prefrontal cortex (dlPFC) - middle frontal sulcus, and 8 ROIs located outside the brain/head of the subject (one ROI in each corner of the scanned volume). These control ROIs enabled us to demonstrate the specificity of the results to the visuomotor cortices. The choice of dlPFC as a control area was motivated by its proximity to the premotor areas and lack of task-related activity.

Intertrial fMRI variability. Variability across trials was computed for each subject separately, relative to their mean hemodynamic response in each ROI. We estimated a hemodynamic response function (HRF) for each subject, ROI, and target by computing the mean response across all trials to a given target. Then, we built a general linear model (GLM) with a row for every time-point and a column for every trial. Each column contained a delta function at the time point corresponding to the go cue (movement onset), which was convolved with the HRF described above. This enabled us to estimate a response amplitude (beta value) for each trial using multiple regression. Note that by using individual subject HRFs for this analysis, we were able to entirely discount the mean HRF amplitude and shape from our estimates – yielding a pure (isolated) measure of individual intertrial variability relative to the mean.

Intertrial fMRI variability was estimated as the standard deviation across beta values (trials) to each of the targets. Before examining the correlations of individual fMRI variability magnitudes across targets and arms, we first regressed-out the subjects' framewise displacement magnitudes. This ensured that individual fMRI variability measures were not generated by potential differences in head motion (Power et al., 2012).

Correlations. We used Pearson correlation coefficients to assess whether individual kinematic variability magnitudes were correlated across targets, arms, and different kinematic components. Equivalent analyses were performed to examine whether individual fMRI variability magnitudes (in each of the examined ROIs) were correlated across targets and arms as well as between the variability of each kinematic component and fMRI variability in each ROI. We assessed the statistical significance using a permutation tests. We randomly shuffled the variability values of the different subjects in each correlation analysis and computed the correlation. This process was repeated 5000 times to generate 5000 correlation values that represented a distribution of

correlations expected by chance (null distribution). For the true (un-shuffled) value to be considered 212
significant, it had to surpass the 97.5th percentile of the null distribution (i.e., the equivalent of a $p <$ 213
0.05 value in a two-tailed t-test). We used the false discovery rate (FDR) correction (Benjamini and 214
Hochberg, 1995; Yekutieli and Benjamini, 1999) to correct for the multiple comparisons across 215
target pairs and across ROIs. 216

Searchlight analysis. In addition to the ROI analysis, we used a searchlight analysis (Kriegeskorte et 217
al., 2006) to map the correlations between fMRI variability and kinematic variability (i.e., movement 218
extent, peak velocity, or direction) throughout the entire cortex. Clusters of 125 functional voxels 219
were defined using a cube with an edge length of 5 voxels around each gray matter voxel in the 220
native space of each subject. fMRI variability was calculated for each cluster of voxels, as described 221
above in the ROI analysis. After computing the variability map of each subjects, all maps were 222
transformed to a standard cortical surface using Freesurfer, and correlation analysis between 223
kinematic and fMRI variabilities were performed for each kinematic measure using movements 224
performed by either right or left arm. This yielded six correlation maps (three kinematic variables 225
and two arms). A student t-test was used to determine the significance of the correlation across 226
subjects in each vertex. We used FDR correction to correct for the multiple comparisons performed 227
across vertices (Storey, 2002). 228

RESULTS 229*Intertrial kinematic Variability.* 230

Subjects exhibited considerable intertrial kinematic variability in their slice (out-and-back) 231
 movements to each of the four targets (Figure 1B). We focused our analyses on three kinematic 232
 components: direction (at end-point) and extent, which are commonly reported in behavioral studies 233
 (Gordon et al., 1994b; Krakauer et al., 2000; van Beers, 2009), and peak velocity, which is 234
 commonly reported in electrophysiology studies (Churchland et al., 2006; Cisek, 2006). Note that 235
 movement extent and peak velocity are mutually dependent, because peak velocity scales with 236
 increasing target distance (Gordon et al., 1994a). 237

In line with previous findings, we found that the variance of movement extent and peak 238
 velocity grew with the mean (correlation across subjects: $r = 0.35$ and $r = 0.53$ respectively, averaged 239
 across targets and arms). To examine differences in intertrial variability not explained by differences 240
 in the mean, we used the coefficient of variation (CV). In contrast, mean movement direction was 241
 not correlated with its standard deviation across trials ($r < 0.1$). There was, therefore, no reason to 242
 normalize this measure, so we used the standard deviation (SD) across trials to quantify movement 243
 direction variability. 244

When examining each of the kinematic components separately, individual subjects exhibited 245
 consistent magnitudes of intertrial variability across movements to different targets (Figure 2A&B). 246
 Thus, subjects who were, for example, more variable in their movement extents to one target tended 247
 to be more variable in their movement extents to all other targets. We quantified this by computing 248
 the mean Pearson correlation coefficients across all target pairs for movements performed with the 249
 right arm ($r = 0.29, 0.41, \text{ and } 0.39$ for movement direction, extent, and peak velocity respectively, 250
 $q(\text{FDR}) < 0.001$) and left arm ($r = 0.46, 0.58, \text{ and } 0.40$ for movement direction, extent, and peak 251
 velocity respectively, $q(\text{FDR}) < 0.001$). Significant correlations were also evident when comparing 252
 the variability magnitudes of each kinematic component across arms (Figure 2C). For example, 253
 subjects with more variable movement extents in right arm movements exhibited more variable 254
 movement extents in left arm movements as well ($r = 0.65, 0.67, \text{ and } 0.55$ for movement direction, 255
 extent, and peak velocity, $p < 0.001$). 256

In line with previous reports (Gordon et al., 1994a), intertrial variability of movement extent 257
and peak velocity were strongly correlated in movements of the right arm ($r = 0.73$, $p < 0.001$; 258
Figure 2D) and left arm ($r = 0.87$, $p < 0.001$; Figure 2E), but variability of movement extent and 259
movement direction (right arm: $r = 0.06$, $p = 0.37$; left arm: $r = 0.27$, $p = 0.07$) or peak velocity and 260
movement direction (right arm: $r = -0.06$, $p = 0.62$; left arm: $r = 0.17$, $p = 0.17$) were not. Thus, 261
individuals who exhibited large movement extent and peak velocity variabilities did not necessarily 262
exhibit large movement direction variability and vice versa. 263

Intertrial fMRI variability

 264

All subjects exhibited robust fMRI responses during the execution of movements, which 265
enabled us to identify six cortical ROIs that are commonly examined in motor system studies (Figure 266
3): Primary Motor Cortex (M1), dorsal premotor cortex (PMd), ventral premotor cortex (PMv), 267
supplementary motor area (SMA), superior parietal lobule (SPL), and inferior parietal lobule (IPL). 268
In addition to the motor ROIs we also identified ROIs in early visual cortex (Vis), dorsolateral 269
prefrontal cortex (dlPFC), and outside the brain (OOB). 270

We then quantified intertrial fMRI variability in each of the ROIs, separately for each 271
subject, in the following manner: First, we estimated the hemodynamic response function (HRF) in 272
each ROI for each target by averaging the fMRI responses across all movements to that target 273
(Figure 4A). We then used the target-specific HRF in a GLM analysis to estimate a response 274
amplitude/beta-value for each trial/movement in the experiment (Figure 4B). Note that using a 275
target-specific HRF enabled us to compute single trial responses/beta-values relative to the mean 276
HRF of each subject. This approach discounted potential between-subject differences in the mean 277
amplitude and shape of individual HRFs. Finally, we quantified intertrial fMRI variability by 278
computing the standard deviation across beta-values for each of the targets (Figure 4B&C). 279

Intertrial fMRI variability was correlated across all pairs of targets in most of the examined 280
ROIs (Figure 5A). Hence, subjects who exhibited more variable brain responses when moving to one 281
target also exhibited more variable brain responses when moving to other targets. During right arm 282
movements all ROIs in the left hemisphere except dlPFC, and all ROIs in the right hemisphere 283
except PMd and dlPFC, exhibited significant pair-wise correlations across targets ($r > 0.32$, $q(\text{FDR})$ 284

< 0.05). Correlations in the dlPFC and out of brain (OOB) ROIs were not significant ($r < 0.26$, $q(\text{FDR}) > 0.1$). Taken together, these findings demonstrate that correlation in fMRI variability magnitudes across targets was specific to cortical ROIs that were activated by the task. Note that early visual cortex was weakly activated in this task by the presentation of the target location at the beginning of each trial and the presentation of the go cue 5 seconds later. The significant correlations across targets in early visual cortex demonstrate that some subjects exhibited larger intertrial fMRI variability in visual cortex than others, regardless of the movement's target. This phenomena was recently demonstrated by our lab (Arazi et al., 2017a, 2017b). Similar results were also apparent for left arm movements (data not shown).

Individual magnitudes of fMRI variability were also significantly correlated across right and left arm movements in many of the examined motor ROIs (Figure 5B). This was evident in all ROIs in the left hemisphere ($r > 0.43$, $q(\text{FDR}) < 0.05$; Figure 5B, red bars) except for M1 and dlPFC, and in the SPL, PMd, and SMA in the right hemisphere ($r > 0.47$, $q(\text{FDR}) < 0.05$; Figure 5B, yellow bars). In addition, fMRI variability magnitudes were significantly correlated across left and right arm movements in contralateral SPL, PMd, and SMA ROIs ($r > 0.48$, $q(\text{FDR}) < 0.05$; Figure 5B, purple bars). This means that, for example, variability in left PMd during right arm movements was significantly correlated with variability in right PMd during left arm movements. Note that consistent fMRI variability across targets and hands was mostly apparent in parietal and prefrontal motor areas, yet was entirely absent in M1. Correlations in the dlPFC and out of brain (OOB) ROIs were not significant ($r < 0.33$, $q(\text{FDR}) > 0.09$). This demonstrates that consistent fMRI variability differences across subjects were not due to differences in scanner measurement noise across subjects. Such scanner noise differences would be apparent in multiple ROIs and even in ROIs located outside the brain.

Relationship between kinematic and fMRI variability

Subjects with larger intertrial fMRI variability in the IPL exhibited larger intertrial extent variability (Figure 6). We examined to what extent between-subject differences in kinematic variability could be explained by fMRI variability measures in right and left ROIs using partial least squares regression. We performed this analysis separately for right and left hand movements and

then averaged across hands. Intertrial fMRI variability in right and left IPL explained 24% ($q(\text{FDR}) = 0.004$) of the between-subject differences in extent variability, 15% of the variability in the peak velocity, and 8% of the variability in movement direction. The IPL was the only ROI where there was a significant relationship between fMRI variability magnitudes and any of the kinematic variability measures. In contrast, intertrial fMRI variability in M1 explained only 2%, 5%, and 4% ($q(\text{FDR}) > 0.5$) of the between-subject differences in direction, extent, and peak velocity variability respectively. Correlations were not significant in all the control ROIs (dlPFC and out of brain, $R^2 < 8\%$, $q(\text{FDR}) > 0.2$).

Searchlight analysis

To examine the spatial selectivity of the cortical-kinematic relationship we performed an additional analysis using a whole-brain searchlight approach (Kriegeskorte et al., 2006). We mapped the correlations between kinematic variability magnitudes and fMRI variability magnitudes across the entire cortical surface, so as not to restrict the analysis to a-priori ROIs. We used a volumetric searchlight cube of 125 functional voxels in the cortical gray matter segmented within the native space of each subject. For each searchlight cube, we calculated the intertrial fMRI variability (as described above for the ROIs) and then registered the resulting variability maps of all subjects to a common inflated brain. We calculated Pearson correlation coefficients to estimate the relationship between intertrial fMRI variability magnitudes and variability magnitudes of each kinematic variable: movement extent, peak velocity, and direction.

This analysis yielded three searchlight maps that revealed complementary results to those described above. We did not find any cortical areas where fMRI variability magnitudes were significantly correlated with variability magnitudes in movement direction or peak velocity. Significant positive correlations, however, were found in bi-lateral inferior parietal cortex when examining movement extent (Figure 7). Note that the searchlight map is highly symmetric across hemispheres and is relatively similar across movements of the right (Figure 7, Red) and left (Figure 7, Blue) arms.

Alternative sources of fMRI variability

Between subject differences in fMRI variability can be generated by several non-neural 340
sources that need to be considered. First, previous studies of fMRI variability have reported that the 341
strength of the mean fMRI response was correlated with the magnitude of intertrial variability across 342
subjects (He, 2013; Ferri et al., 2015). To measure intertrial fMRI variability in individual subjects 343
independently of their mean response, we estimated intertrial variability with respect to the mean 344
hemodynamic response function (HRF) apparent in each ROI of each subject (see methods). This 345
enabled us to compute the relative fMRI variability with respect to the actual HRF as opposed to 346
using a canonical HRF that assumes an identical shape and amplitude across subjects. Indeed, when 347
using this method, intertrial fMRI variability was not correlated significantly with mean fMRI 348
response in any of the ROIs ($r < 0.15$, $p > 0.1$). 349

Second, we regressed-out the mean fMRI time-courses of the lateral ventricles and an ROI 350
containing all gray-matter voxels (i.e., “global component”). These time-courses represent fMRI 351
fluctuations that may, in part, be associated with changes in respiration, blood pressure, and other 352
non-neural origins. 353

Third, head-motion artifacts can generate fMRI variability across trials. To ensure that our 354
results were not generated by head-motion artifacts, we regressed-out estimated head-motion 355
parameters from the fMRI activity of each voxel in the brain before performing the analyses (see 356
methods). Furthermore, we also computed the mean framewise displacement across head-motion 357
parameters (i.e., the mean amount of head motion across samples/TRs) for each subject. We 358
regressed-out individual values of framewise displacement from the fMRI variability magnitudes 359
before examining correlations across targets and/or arms. This ensured that the reported between- 360
subject differences in fMRI variability magnitudes were not generated by underlying differences in 361
head motion across subjects. 362

DISCUSSION

363

Our results reveal that individual subjects exhibit distinct magnitudes of kinematic variability, which are consistent across movements to different locations when performed by either arm. Individual variability magnitudes in movement extent, peak velocity, or direction were strongly correlated across different targets and across arms (Figure 2). This means that an individual who exhibits large movement extent variability to one target is likely to exhibit large movement extent variability to all other targets regardless of the arm that the subject uses to perform the movements.

Analogous findings were also apparent when examining fMRI variability magnitudes of individual subjects (Figures 5). Subjects with larger fMRI variability magnitudes in most of the examined motor areas tended to exhibit larger variability regardless of target location or arm used to perform the movements. A surprising exception was M1, where fMRI variability magnitudes were not consistent across arms. This suggests that cortical variability magnitudes in parietal and premotor motor system areas are relatively stable individual characteristics, while cortical variability magnitudes in M1 may represent more transient states that change with the choice of effector or task.

The results also revealed a specific relationship between variability magnitudes in one of the kinematic measures, movement extent, and cortical variability magnitudes in one brain area, the IPL. Indeed, fMRI variability magnitudes in the IPL explained 24% of the differences in movement-extent variability across subjects. In contrast, fMRI variability magnitudes in M1 explained only 5% of between-subject differences in movement-extent variability (Figure 6). The specificity of these results was further validated by a searchlight analysis that revealed significant correlations between the kinematic and cortical variability magnitudes only with respect to movement extent and only in IPL (Figure 7). Parietal cortex is thought to play key roles in motor planning, sensory motor mapping, and state estimation (Buneo and Andersen, 2006). We, therefore, suggest that a considerable portion of movement-extent variability is generated by cortical variability associated with movement preparation, rather than cortical variability associated with movement execution.

Note that this is the first study to ever examine the consistency of kinematic variability across targets/hand and relate it with cortical response variability in humans. Contemporary models of motor control and motor learning (Pekny et al., 2015; Wolpert and Flanagan, 2016) emphasize the

importance of intertrial-variability for motor system flexibility and accuracy. For example, it has
been reported that individuals with larger intertrial behavioral variability learn new motor tasks more
quickly (Wu et al., 2014). Note that while larger intertrial-variability may be useful for flexibility
and learning, variability in movement accuracy across trials is often detrimental. We, therefore,
speculate that the stable between-subject differences in cortical and kinematic variability magnitudes
described here are likely to predispose individual subjects to exhibit different motor capabilities.

Neural sources of kinematic variability

Previous theories have suggested that intertrial kinematic variability is predominantly
generated by the variable activity of sensory neural populations (Osborne et al., 2005; for review, see
Lisberger and Medina, 2015), PMd and M1 neural populations involved in motor planning
(Churchland et al., 2006), or by neuro-muscular variability that characterizes actual movement
execution (van Beers et al., 2004; van Beers, 2009). It is entirely possible, however, that different
sources of neural variability generate kinematic variability under different experimental conditions,
such that behavioral motor variability would embody the sum of multiple neural variability sources
(for review see Faisal et al., 2008). With this in mind, neural variability in a particular brain area is
likely to explain a certain proportion of kinematic variability. Furthermore, neural variability in
different brain areas may generate variability in different kinematic components of movements (e.g.,
movement extent versus movement direction).

Our results indeed demonstrate that about a quarter of the between-subject differences in
movement extent variability are explained by individual neural variability differences in parietal
cortex, which is thought to play a dominant role in the planning and preparation of reaching
movements (Cohen and Andersen, 2002). While previous electrophysiology studies have reported
that variability in M1 and PMd neural activity (during preparation for movement) generates
variability in peak movement velocity (Churchland et al., 2006; Chaisanguanthum et al., 2014), our
results suggest that stronger relationships between neural and kinematic variability will be evident in
parietal brain areas and particularly in IPL (Figure 6&7).

It may seem surprising that correlations between kinematic variability and fMRI variability
were weak in M1 given that it is the lowest area in the cortical motor hierarchy (e.g., Shadmehr and

Krakauer, 2008). In humans, however, only 30% to 40% of the axons in the corticospinal tract 419
originate from neurons in M1, while the rest originate from the premotor, supplementary motor, and 420
posterior parietal cortices (Kandel et al., 2013). This means that neural variability in parietal regions 421
may potentially generate kinematic variability downstream of M1, in spinal motor circuits. A 422
potentially interesting analogy can be found in songbirds where the lateral magnocellular nucleus of 423
anterior nidopallium has evolved to inject direct neural variability into the motor circuits that control 424
singing – apparently enabling juvenile birds to learn through trial and error (Ölveczky et al., 2011). 425

Parietal cortex contains neural populations that perform a wide variety of computations that 426
are essential for motor control including motor planning, sensory-motor mapping, and state 427
estimation (Wolpert and Ghahramani, 2000; Cohen and Andersen, 2002; Buneo and Andersen, 428
2006; Churchland et al., 2006; Shadmehr and Krakauer, 2008). More specifically, neural populations 429
in the IPL are thought to integrate high-order sensory and motor information in support of high-level 430
motor functions (Fogassi and Luppino, 2005), and represent conscious motor intentions (Desmurget 431
and Sirigu, 2012). Within all of these frameworks, each with its specific mechanistic focus, 432
variability in the activity of parietal neural populations would generate variability in the kinematics 433
of executed movements. 434

An alternative interpretation of our results might emphasize the sensory roles of parietal 435
cortex. In this case the causality would be reversed such that the measured fMRI variability would 436
be generated by movement variability (and not the other way around). While it is difficult to entirely 437
rule this option out, it is important to note that we did not find significant correlations between any 438
of the kinematic measures and fMRI variability magnitudes in somatosensory cortices (Figure 7). 439
The selectivity of the results to IPL argues against such a sensory driven explanation of the results. 440

Finally, it is important to note that we and all previous electrophysiology studies on the topic 441
measured variability only in the kinematics of the movements and not in their dynamics. It is highly 442
possible that intertrial-variability in movement dynamics (i.e., muscle activation), which are not 443
necessarily captured in measures of kinematic variability, may be explained by intertrial neural 444
variability in specific brain areas. 445

Decomposing neural variability 446

Neural variability is likely to arise from a wide variety of molecular and cellular mechanisms that govern neural transduction and transmission in addition to mechanisms that govern neural network dynamics. While it is difficult to disentangle the different sources of neural variability using neuroimaging, it is possible to decompose variability into different spatial and temporal components using measures from different types of neuroimaging and electrophysiological techniques (Dinstein et al., 2015). When studying variability with fMRI, it is possible to simultaneously quantify intertrial-variability in multiple different brain areas, but the temporal resolution of this measure is limited by the sluggish nature of the hemodynamic response (Heeger and Ress, 2002). Furthermore, since fMRI is not a direct measure of neural activity, but rather a measure of hemodynamic changes over time, intertrial-variability in the function of neuro-vascular coupling mechanisms will be an inherent part of the fMRI intertrial-variability measure. This limits the ability to measure neural variability with fMRI and, therefore, limits the ability to relate neural variability and behavioral variability measures. With this in mind it is impressive that we were able to identify a consistent relationship between fMRI variability and movement extent variability which was similarly evident in movements of right and left arm (Figure 6&7). We speculate that stronger relationships may be revealed with direct measures of human neural activity such as ECOG recordings.

Hemispheric lateralization

While arm movements are clearly generated and controlled by neural activity in the contralateral hemisphere (Penfield and Boldrey, 1937), human fMRI studies show activity and even directional selectivity of arm movement (Fabbri et al., 2010; Haar et al., 2015) across the cortical motor hierarchy in the ipsilateral hemisphere. Here, we found significant correlations between movement extent variability and neural variability in both the contralateral and ipsilateral hemispheres. We speculate that neural variability in both hemispheres may, therefore, have an impact on the accuracy and reliability of arm movements.

Conclusions

This study demonstrates that kinematic variability and parietal and pre-frontal cortical variability are stable individual traits, which appear consistently across movements to different

targets when performed by either arm. Furthermore, these variabilities are related such that subjects 475
with larger neural variability in IPL exhibited larger movement-extent variability. We believe that 476
these results represent an important first step for understanding how neural variability may generate 477
movement variability in humans and, thereby, predispose individuals to exhibit distinct motor 478
capabilities such as motor learning proficiency. 479

REFERENCES	480
Arazi A, Censor N, Dinstein I (2017a) Neural Variability Quenching Predicts Individual Perceptual Abilities. <i>J Neurosci</i> 37:97–109 Available at: http://www.ncbi.nlm.nih.gov/pubmed/28053033 [Accessed July 18, 2017].	481 482 483
Arazi A, Gonen-Yaacovi G, Dinstein I (2017b) Trial-by-trial neural variability is a stable individual trait of adult humans. <i>bioRxiv</i> Available at: https://doi.org/10.1101/096198 .	484 485
Benjamini Y, Hochberg Y (1995) Controlling the false discovery rate: a practical and powerful approach to multiple testing. <i>J R Stat Soc B</i> 57:289–300 Available at: http://www.stat.purdue.edu/~doerge/BIOINFORM.D/FALL06/Benjamini and Y FDR.pdf http://engr.case.edu/ray_soumya/mlrg/controlling_fdr_benjamini95.pdf .	486 487 488 489
Braun D a, Aertsen A, Wolpert DM, Mehring C (2009) Motor Task Variation Induces Structural Learning. <i>Curr Biol</i> 19:352–357 Available at: http://www.pubmedcentral.nih.gov/articlerender.fcgi?artid=2669412&tool=pmcentrez&rendertype=abstract [Accessed December 1, 2014].	490 491 492 493
Buneo CA, Andersen RA (2006) The posterior parietal cortex: Sensorimotor interface for the planning and online control of visually guided movements. <i>Neuropsychologia</i> 44:2594–2606.	494 495
Chaisanguanthum KS, Shen HH, Sabes PN (2014) Motor variability arises from a slow random walk in neural state. <i>J Neurosci</i> 34:12071–12080 Available at: http://www.ncbi.nlm.nih.gov/pubmed/25186752 [Accessed September 5, 2014].	496 497 498
Churchland MM, Abbott LF (2012) Two layers of neural variability. <i>Nat Neurosci</i> 15:1472–1474 Available at: http://www.ncbi.nlm.nih.gov/pubmed/23103992 [Accessed December 9, 2014].	499 500
Churchland MM, Afshar A, Shenoy K V. (2006) A Central Source of Movement Variability. <i>Neuron</i> 52:1085–1096 Available at: http://www.pubmedcentral.nih.gov/articlerender.fcgi?artid=1941679&tool=pmcentrez&rendertype=abstract [Accessed November 26, 2014].	501 502 503 504
Cisek P (2006) Preparing for speed. Focus on “Preparatory activity in premotor and motor cortex reflects the speed of the upcoming reach.” <i>J Neurophysiol</i> 96:2842–2843 Available at: http://www.ncbi.nlm.nih.gov/pubmed/16928790 [Accessed July 25, 2016].	505 506 507
Cohen YE, Andersen RA (2002) A common reference frame for movement plans in the posterior parietal cortex. <i>Nat Rev Neurosci</i> 3:553–562 Available at: http://www.nature.com/doi/10.1038/nrn873 [Accessed September 15, 2016].	508 509 510
Desmurget M, Sirigu A (2012) Conscious motor intention emerges in the inferior parietal lobule. <i>Curr Opin Neurobiol</i> 22:1004–1011 Available at: http://www.sciencedirect.com/science/article/pii/S0959438812001298 [Accessed May 17, 2017].	511 512 513
Destrieux C, Fischl B, Dale A, Halgren E (2010) Automatic parcellation of human cortical gyri and sulci using standard anatomical nomenclature. <i>Neuroimage</i> 53:1–15.	514 515
Dinstein I, Heeger DJ, Behrmann M (2015) Neural variability: friend or foe? <i>Trends Cogn Sci</i> 19:322–328 Available at: http://www.sciencedirect.com/science/article/pii/S1364661315000911 [Accessed February 24, 2016].	516 517 518
Fabbri S, Caramazza A, Lingnau A (2010) Tuning curves for movement direction in the human visuomotor system. <i>J Neurosci</i> 30:13488–13498 Available at: http://www.jneurosci.org/content/30/40/13488.short [Accessed December 5, 2014].	519 520 521
Faisal a A, Selen LPJ, Wolpert DM (2008) Noise in the nervous system. <i>Nat Rev Neurosci</i> 9:292–303 Available at: http://www.pubmedcentral.nih.gov/articlerender.fcgi?artid=2631351&tool=pmcentrez&rendertype=abstract	522 523 524

bstract [Accessed July 10, 2014].	525
Faul F, Erdfelder E, Buchner A, Lang A-G (2009) Statistical power analyses using G*Power 3.1: tests for correlation and regression analyses. <i>Behav Res Methods</i> 41:1149–1160 Available at: http://www.springerlink.com/index/10.3758/BRM.41.4.1149 [Accessed February 21, 2017].	526 527 528
Ferri F, Costantini M, Huang Z, Perrucci MG, Ferretti A, Romani GL, Northoff G (2015) Intertrial Variability in the Premotor Cortex Accounts for Individual Differences in Peripersonal Space. <i>J Neurosci</i> 35:16328–16339 Available at: http://www.jneurosci.org.329.han.sub.uni-goettingen.de/content/35/50/16328.full .	529 530 531 532
Fischl B (2012) FreeSurfer. <i>Neuroimage</i> 62:774–781.	533
Fogassi L, Luppino G (2005) Motor functions of the parietal lobe. <i>Curr Opin Neurobiol</i> 15:626–631 Available at: http://www.sciencedirect.com/science/article/pii/S0959438805001649 [Accessed May 17, 2017].	534 535
Gordon J, Ghilardi MF, Cooper SE, Ghez C (1994a) Accuracy of planar reaching movements. II. Systematic extent errors resulting from inertial anisotropy. <i>Exp Brain Res</i> 99:112–130.	536 537
Gordon J, Ghilardi MF, Ghez C (1994b) Accuracy of planar reaching movements. I. Independence of direction and extent variability. <i>Exp brain Res</i> 99:97–111 Available at: http://www.ncbi.nlm.nih.gov/pubmed/7925800 [Accessed February 14, 2016].	538 539 540
Haar S, Donchin O, Dinstein I (2015) Dissociating Visual and Motor Directional Selectivity Using Visuomotor Adaptation. <i>J Neurosci</i> 35:6813–6821 Available at: http://www.jneurosci.org./content/35/17/6813.full [Accessed April 30, 2015].	541 542 543
Harbourne RT, Stergiou N (2009) Movement variability and the use of nonlinear tools: principles to guide physical therapist practice. <i>Phys Ther</i> 89:267–282 Available at: http://www.pubmedcentral.nih.gov/articlerender.fcgi?artid=2652347&tool=pmcentrez&rendertype=a bstract [Accessed November 24, 2014].	544 545 546 547
He BJ (2013) Spontaneous and task-evoked brain activity negatively interact. <i>J Neurosci</i> 33:4672–4682 Available at: http://www.jneurosci.org/content/33/11/4672.full .	548 549
Heeger DJ, Ress D (2002) What Does fMRI Tell Us About Neuronal Activity? <i>Nat Rev Neurosci</i> 3:142–151 Available at: http://www.ncbi.nlm.nih.gov/pubmed/11836522 [Accessed October 25, 2016].	550 551
Herzfeld DJ, Shadmehr R (2014) Motor variability is not noise, but grist for the learning mill. <i>Nat Neurosci</i> 17:149–150 Available at: http://www.ncbi.nlm.nih.gov/pubmed/24473260 [Accessed November 14, 2014].	552 553 554
Kandel ER, Schwartz JH, Jessell TM (2013) Principles of Neural Science. Available at: http://www.amazon.com/Principles-Neural-Science-Eric-Kandel/dp/0838577016 .	555 556
Kao MH, Doupe AJ, Brainard MS (2005) Contributions of an avian basal ganglia-forebrain circuit to real-time modulation of song. <i>Nature</i> 433:638–643.	557 558
Krakauer JW, Pine Z, Ghilardi M, Ghez C (2000) Learning of visuomotor transformations for vectorial planning of reaching trajectories. <i>J Neurosci</i> 20:8916–8924 Available at: http://www.jneurosci.org/content/20/23/8916.short [Accessed December 4, 2014].	559 560 561
Kriegeskorte N, Goebel R, Bandettini P (2006) Information-based functional brain mapping. <i>Proc Natl Acad Sci U S A</i> 103:3863–3868 Available at: http://dx.doi.org/10.1073/pnas.0600244103 .	562 563
Latash ML, Scholz JP, Schöner G (2007) Toward a new theory of motor synergies. <i>Motor Control</i> 11:276–308 Available at: http://www.ncbi.nlm.nih.gov/pubmed/17715460 .	564 565
Lisberger SG, Medina JF (2015) How and why neural and motor variation are related. <i>Curr Opin Neurobiol</i> 33:110–116 Available at: http://dx.doi.org/10.1016/j.conb.2015.03.008 .	566 567

Mandelblat-Cerf Y, Paz R, Vaadia E (2009) Trial-to-trial variability of single cells in motor cortices is dynamically modified during visuomotor adaptation. <i>J Neurosci</i> 29:15053–15062 Available at: http://www.ncbi.nlm.nih.gov/pubmed/19955356 [Accessed November 25, 2014].	568 569 570
Ölveczky BP, Otchy TM, Goldberg JH, Aronov D, Fee MS (2011) Changes in the neural control of a complex motor sequence during learning. <i>J Neurophysiol</i> 106:386–397 Available at: http://www.pubmedcentral.nih.gov/articlerender.fcgi?artid=3129720&tool=pmcentrez&rendertype=abstract [Accessed December 2, 2014].	571 572 573 574
Osborne LC, Lisberger SG, Bialek W (2005) A sensory source for motor variation. <i>Nature</i> 437:412–416 Available at: http://www.pubmedcentral.nih.gov/articlerender.fcgi?artid=2551316&tool=pmcentrez&rendertype=abstract [Accessed October 26, 2014].	575 576 577 578
Pekny SE, Izawa J, Shadmehr R (2015) Reward-dependent modulation of movement variability. <i>J Neurosci</i> 35:4015–4024 Available at: http://www.ncbi.nlm.nih.gov/pubmed/25740529 .	579 580
Penfield W, Boldrey E (1937) Somatic Motor and Sensory Representation in the Cerebral Cortex of Man as Studies by Electrical Stimulation. <i>Brain</i> 60:389–443 Available at: http://brain.oxfordjournals.org/cgi/doi/10.1093/brain/60.4.389 [Accessed November 24, 2016].	581 582 583
Power JD, Barnes KA, Snyder AZ, Schlaggar BL, Petersen SE (2012) Spurious but systematic correlations in functional connectivity MRI networks arise from subject motion. <i>Neuroimage</i> 59:2142–2154 Available at: http://www.sciencedirect.com/science/article/pii/S1053811911011815 [Accessed May 18, 2017].	584 585 586
Sauerbrei BA, Lubenov E V, Siapas AG (2015) Structured Variability in Purkinje Cell Activity during Locomotion. <i>Neuron</i> 87:840–852 Available at: http://www.sciencedirect.com/science/article/pii/S0896627315006789 [Accessed March 5, 2016].	587 588 589
Schmidt R a, Zelaznik H, Hawkins B, Frank JS, Quinn JT (1979) Motor-output variability: a theory for the accuracy of rapid motor acts. <i>Psychol Rev</i> 47:415–451.	590 591
Shadmehr R, Krakauer JW (2008) A computational neuroanatomy for motor control. <i>Exp Brain Res</i> 185:359–381 Available at: http://link.springer.com/article/10.1007/s00221-008-1280-5 [Accessed December 3, 2014].	592 593 594
Stein RB, Gossen ER, Jones KE (2005) Neuronal variability: noise or part of the signal? <i>Nat Rev Neurosci</i> 6:389–397 Available at: http://www.ncbi.nlm.nih.gov/pubmed/15861181 [Accessed July 15, 2014].	595 596
Storey JD (2002) A direct approach to false discovery rates. <i>J R Stat Soc Ser B Stat Methodol</i> 64:479–498.	597
Teo JTH, Swayne OBC, Cheeran B, Greenwood RJ, Rothwell JC (2011) Human theta burst stimulation enhances subsequent motor learning and increases performance variability. <i>Cereb Cortex</i> 21:1627–1638 Available at: http://www.ncbi.nlm.nih.gov/pubmed/21127013 [Accessed November 17, 2014].	598 599 600
Todorov E (2004) Optimality principles in sensorimotor control. <i>Nat Neurosci</i> 7:907–915 Available at: http://www.pubmedcentral.nih.gov/articlerender.fcgi?artid=1488877&tool=pmcentrez&rendertype=abstract .	601 602 603
van Beers RJ (2009) Motor Learning Is Optimally Tuned to the Properties of Motor Noise. <i>Neuron</i> 63:406–417 Available at: http://www.ncbi.nlm.nih.gov/pubmed/19679079 [Accessed November 29, 2014].	604 605
van Beers RJ, Haggard P, Wolpert DM (2004) The role of execution noise in movement variability. <i>J Neurophysiol</i> 91:1050–1063 Available at: http://www.ncbi.nlm.nih.gov/pubmed/14561687 [Accessed December 5, 2014].	606 607 608
Wilson C, Simpson SE, van Emmerik RE a, Hamill J (2008) Coordination variability and skill development in expert triple jumpers. <i>Sports Biomech</i> 7:2–9 Available at: http://www.ncbi.nlm.nih.gov/pubmed/18341132 [Accessed December 9, 2014].	609 610 611
Wolpert DM, Flanagan JR (2016) Computations underlying sensorimotor learning. <i>Curr Opin Neurobiol</i> 37:7–	612

11 Available at: http://dx.doi.org/10.1016/j.conb.2015.12.003 .	613
Wolpert DM, Ghahramani Z (2000) Computational principles of movement neuroscience. <i>Nat Neurosci</i> 3:1212–1217 Available at: http://www.nature.com/doifinder/10.1038/81497 [Accessed May 16, 2017].	614 615
Woolley SC, Kao MH (2015) Variability in action: Contributions of a songbird cortical-basal ganglia circuit to vocal motor learning and control. <i>Neuroscience</i> 296:39–47 Available at: http://www.sciencedirect.com/science/article/pii/S0306452214008720 [Accessed April 10, 2016].	616 617 618
Wu HG, Miyamoto YR, Gonzales Castro LN, Ölveczky BC, Smith MA (2014) Temporal structure of motor variability is dynamically regulated and predicts motor learning ability. <i>Nat Neurosci</i> 17:312–321 Available at: http://www.ncbi.nlm.nih.gov/pubmed/24413700 [Accessed July 22, 2014].	619 620 621
Yekutieli D, Benjamini Y (1999) Resampling-based false discovery rate controlling multiple test procedures for correlated test statistics. <i>J Stat Plan Inference</i> 82:171–196.	622 623
	624

FIGURE LEGENDS

Figure 1. (A) *Experimental setup.* (B) Representative example of movement paths of one subject. Different colors represent slice movements to the four targets.

Figure 2. *Kinematic variability correlations.* We computed the intertrial variability of movement direction (green), extent (dark blue), and peak velocity (light blue) across movements to each target for each of the subjects. (A) Individual magnitudes of intertrial variability were strongly correlated across the two proximal targets (i.e., regardless of direction). (B) Means and SEM of the Pearson correlations of the variability across all pairs of targets. Significant correlations are marked with asterisks. (C) Scatter plots of the kinematic variability, averaged across targets, of the right and left arms. Each data point represents variability of movements of a single subject. (D,E) Scatter plots of the kinematic variability, averaged across targets, of the right (D) and the left (E) arms. For all scatter plots: data points represent different subjects; lines represent linear fits. Significant correlations are marked with red asterisks.

Figure 3. *Cortical activation during movement execution.* Cortical areas that exhibited larger responses during movement than rest are shown in red/orange. Results were calculated across all subjects (random-effects GLM) and displayed on inflated hemispheres of a template brain. The general locations of the selected ROIs are noted (actual ROIs were anatomically and functionally defined in each subject – see Methods): Primary motor cortex (M1), dorsal premotor cortex (PMd), ventral premotor cortex (PMv), supplementary motor area (SMA), inferior parietal lobule (IPL), superior parietal lobule (SPL), dorsolateral prefrontal cortex (dlPFC), and early visual cortex (Vis).

Figure 4. *fMRI Variability.* Examples of intertrial fMRI variability as quantified in left M1 of 3 subjects during right arm movements. (A) Single trial fMRI responses from left M1 are presented in z-scored units; color coded according to the different targets, mean HRF across trials (i.e., the HRF used in the GLM analysis) is presented in black. Time point zero corresponds to presentation of the go cue. (B) Boxplots demonstrating the distributions of beta-values per target. (C) Standard deviation (SD) across beta values for each target (color code is the same as in A). The mean SD across targets is represented by the black circle. Each row represents data from a single subject.

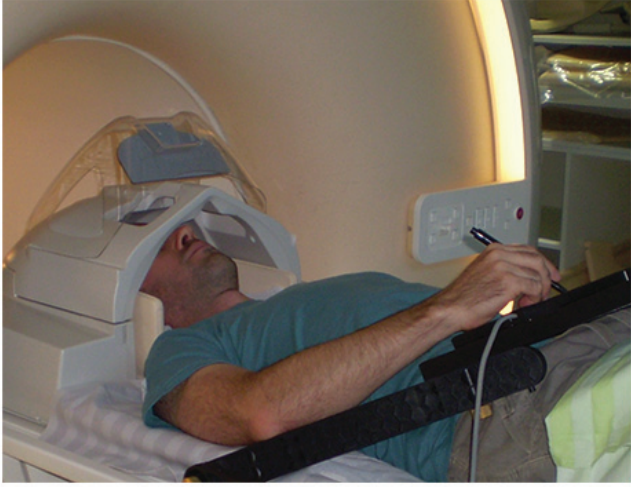
Figure 5. *Cortical variability correlations.* fMRI variability magnitudes during right (A) and left (B) arm movements were correlated across all target pairs. Mean pair-wise correlation coefficients are presented for each left hemisphere (red) and right hemisphere (yellow) ROI. (C) fMRI variability magnitudes were correlated across right and left arm movements in left hemisphere ROIs (red), right hemisphere ROIs (yellow) and in contra-lateral ROIs (purple). Significant correlations are marked with red asterisks.

Figure 6. *Kinematic Variability explained by fMRI Variability.* Multiple regression was performed between fMRI variability magnitudes in each pair of ROIs (right and left hemispheres) and variability magnitudes of each kinematic variable: direction (green), extent (dark blue), or peak velocity (light blue). This analysis was performed separately for right and left hand movements and the results were averaged. Significant explained variance is marked with red asterisks ($q(\text{FDR}) < 0.05$).

Figure 7. *Searchlight analysis* displaying cortical areas with significant correlations between movement extent variability and fMRI variability across subjects. Results for right (red) and left (blue) arm movements are presented on the inflated cortical anatomy of a single subject. Correlation significance was determined based on a student t-test (FDR corrected).

625
626
627
628
629
630
631
632
633
634
635
636
637
638
639
640
641
642
643
644
645
646
647
648
649
650
651
652
653
654
655
656
657
658
659
660
661
662
663
664
665
666
667
668
669
670
671

A



B

